

# Task-free spectral EEG dynamics track and predict patient recovery from severe acquired brain injury



R.L. van den Brink<sup>a,b,c,\*</sup>, S. Nieuwenhuis<sup>a,b</sup>, G.J.M. van Boxtel<sup>d</sup>, G. van Luijtelaar<sup>e</sup>,  
H.J. Eilander<sup>f,g</sup>, V.J.M. Wijnen<sup>d,e,f,h</sup>

<sup>a</sup> Institute of Psychology, Leiden University, Leiden, The Netherlands

<sup>b</sup> Leiden Institute for Brain and Cognition (LIBC), Leiden, The Netherlands

<sup>c</sup> Department of Neurophysiology and Pathophysiology, University Medical Center Hamburg-Eppendorf, Hamburg, Germany

<sup>d</sup> Department of Psychology, Tilburg University, Tilburg, The Netherlands

<sup>e</sup> Donders Institute for Brain, Cognition and Behaviour, Radboud University, Nijmegen, The Netherlands

<sup>f</sup> Libra Rehabilitation Medicine and Audiology, Tilburg, The Netherlands

<sup>g</sup> Radboud University Nijmegen Medical Centre, Department of Primary and Community Care, Nijmegen, The Netherlands

<sup>h</sup> Geriatric Psychiatry Observation Unit, Institution for Mental Health Care 'Dijk and Duin', Parnassia Group, Castricum, Netherlands

## ARTICLE INFO

### Keywords:

Disorders of consciousness

Brain injury

EEG

Classification

## ABSTRACT

For some patients, coma is followed by a state of unresponsiveness, while other patients develop signs of awareness. In practice, detecting signs of awareness may be hindered by possible impairments in the patient's motoric, sensory, or cognitive abilities, resulting in a substantial proportion of misdiagnosed disorders of consciousness. Task-free paradigms that are independent of the patient's sensorimotor and neurocognitive abilities may offer a solution to this challenge. A limitation of previous research is that the large majority of studies on the pathophysiological processes underlying disorders of consciousness have been conducted using cross-sectional designs. Here, we present a study in which we acquired a total of 74 longitudinal task-free EEG measurements from 16 patients (aged 6–22 years, 12 male) suffering from severe acquired brain injury, and an additional 16 age- and education-matched control participants. We examined changes in amplitude and connectivity metrics of oscillatory brain activity within patients across their recovery. Moreover, we applied multi-class linear discriminant analysis to assess the potential diagnostic and prognostic utility of amplitude and connectivity metrics at the individual-patient level. We found that over the course of their recovery, patients exhibited nonlinear frequency band-specific changes in spectral amplitude and connectivity metrics, changes that aligned well with the metrics' frequency band-specific diagnostic value. Strikingly, connectivity during a single task-free EEG measurement predicted the level of patient recovery approximately 3 months later with 75% accuracy. Our findings show that spectral amplitude and connectivity track patient recovery in a longitudinal fashion, and these metrics are robust pathophysiological markers that can be used for the automated diagnosis and prognosis of disorders of consciousness. These metrics can be acquired inexpensively at bedside, and are fully independent of the patient's neurocognitive abilities. Lastly, our findings tentatively suggest that the relative preservation of thalamo-cortico-thalamic interactions may predict the later reemergence of awareness, and could thus shed new light on the pathophysiological processes that underlie disorders of consciousness.

## 1. Introduction

After awakening from coma, some patients remain unresponsive while others show behavioral features that are taken as signs of awareness (Jennett and Plum, 1972; Laureys et al., 2004). The reliance on behavioral criteria for the diagnosis of such disorders of consciousness (DOC) may be suboptimal, because impairments in the patients' motor system can obscure signs of consciousness (Giacino et al., 2014).

These considerations have sparked the development of 'active paradigms' that rely on electroencephalography (EEG) or neuroimaging tools to detect signs of patient awareness during mental tasks (Boly et al., 2011; Fischer et al., 2010; Höller et al., 2011; Kotchoubey et al., 2005; Monti et al., 2010; Owen et al., 2006; Sitt et al., 2014; Wijnen et al., 2007). Though promising, some active paradigms rely on higher-order cognitive abilities such as language comprehension or attention. In addition, putative electrophysiological markers of awareness such as

\* Corresponding author at: Wassenaarseweg 52, 2333AK Leiden, The Netherlands.

E-mail address: [r.l.van.den.brink@fsw.leidenuniv.nl](mailto:r.l.van.den.brink@fsw.leidenuniv.nl) (R.L. van den Brink).

<http://dx.doi.org/10.1016/j.nicl.2017.10.003>

Received 10 March 2017; Received in revised form 19 September 2017; Accepted 2 October 2017

Available online 02 October 2017

2213-1582/ © 2017 The Authors. Published by Elsevier Inc. This is an open access article under the CC BY-NC-ND license (<http://creativecommons.org/licenses/by-nc-nd/4.0/>).

**Table 1**  
Patient characteristics.

P	Ms	M/F	Age	Cause	Initial CT scan (s)*	GCS	T1	T2	T3	LoC1	LoC-discharge	n
1	14	M	19,9	Explosion	Skull fracture, diffuse swelling, high intracranial pressure, intracerebral and contusion haemorrhages, right (sub)cortical, left cortical, and brainstem lesion.	4	25	76	197	3	8	10
2	6	F	22,1	Medulloblastoma	Encephalopathy	?	0	57	70	6	8	1
3	5	M	5,5	Near-drowning	Hypoxia/anoxia, oedema, ischemia, atrophy, diffuse axonal injury	?	6	56	63	3	2	1
4	2	M	17,6	Traffic accident	Epidural haematoma (right)	2t	72	80	139	3	2	7
5	7	M	6	Near-drowning	Hypoxia/anoxia, diffuse axonal injury	3t	8	56	83	3	6	2
6	8	M	20,8	Traffic accident	Punctal haemorrhages, intracerebral haemorrhages, contusion haemorrhages, atrophy, diffuse axonal injury	4	35	60	105	1	2	6
7	4	M	15,4	Traffic accident	Skull fractures, arachnoid haemorrhages, contusion and punctal haemorrhages (right frontal, temporal, parietal), diffuse swelling.	4	33	136	112	2	5	5
8	7	M	20,4	Traffic accident	N.A.	5	28	69	82	5	7	2
9	3	M	25,2	Traffic accident	Skull fracture, oedema and punctal haemorrhages (cortical), diffuse swelling, and diffuse white matter lesions.	2t	65	64	77	2	7	4
10	4	M	8,4	Cerebral haemorrhages	Intraventricular and intracerebral haemorrhages, left cortical.	2t	33	81	119	3	7	5
11	8	F	18,8	Traffic accident	Oedema, ischemia, high intracranial pressure, diffuse swelling.	3	29	49	115	4	6	8
12	3	M	17,5	Traffic accident	Oedema, intraventricular and intracerebral haemorrhages, focal lesions (subcortical, brainstem), diffuse white matter lesions.	4	13	44	92	3	8	3
13	7	M	21,8	Traffic accident	Punctal haemorrhages, intraventricular haemorrhage (left), diffuse swelling, diffuse axonal injury.	5	26	71	105	2	3	8
14	5	F	15,7	Traffic accident	Subarachnoid haemorrhage (right), high intracranial pressure, oedema (right subcortical and brainstem).	4	30	60	99	2	6	7
15	9	M	17,2	Traffic accident	Intraventricular haemorrhages (bilateral), multiple punctal haemorrhages, Large haemorrhage in basal ganglia, and right frontal, oedema (mainly left periventricular white matter).	3	62	80	157	2	5	1
16	4	F	15,2	Pneumonia + sepsis shock	Hypodensity in basal ganglia and cortical temporoparietal, anoxia, cortical and cerebellar atrophy, diffuse white matter lesion.	3	57	102	45	2	4	4

P = patient; Ms. = participated measurements; F = female; M = male; Age = age at injury; \* = diagnoses based on the medical reports of the acute phase; GCS = Glasgow coma scale at admission hospital; t = time at intensive care unit in days; T2 = time before admission to Rehabilitation Centre Leijpark in days; T3 = programme duration Rehabilitation Centre Leijpark in days; LoC1 = level of consciousness during the first EEG measurement; LoC-discharge = level of consciousness at discharge; n = number of measurements for each participant.

the mismatch negativity may be absent in patients that do show behavioral signs of consciousness (Fischer et al., 2010; Höller et al., 2011; Kotchoubey et al., 2005; Wijnen et al., 2007). Moreover, a necessity for active paradigms is that the patients' sensory pathways are intact, which may not always be the case. Thus, diagnostic tools that are independent of the patients' neurocognitive abilities and integrity of sensorimotor pathways may offer a substantial improvement on existing tools.

Accordingly, task-free paradigms, in which the patient is not required to follow instructions or process stimuli, have recently gained traction (Casali et al., 2013; Demertzi et al., 2015; Estraneo et al., 2016; Rosanova et al., 2012; Schorr et al., 2016; Schurjer et al., 2015; Stender et al., 2016). For instance, using positron emission tomography, Stender et al. (2016) were able to predict the presence and later emergence of consciousness in patients with DOC. Similarly, the cortical spread of EEG activity following transcranial magnetic stimulation dissociates patients with unresponsive wakefulness syndrome (UWS) from those in the minimally conscious state (MCS) (Rosanova et al., 2012). However, these paradigms necessitate the use of costly or impractical equipment, and may therefore not offer the most convenient diagnostic procedures. Task-free EEG spectral amplitude and variance metrics have shown promise as diagnostic and prognostic markers (Schorr et al., 2016; Schurjer et al., 2015), but thus far have been limited in their ability to dissociate UWS from MCS patients (Schurjer et al., 2015), and provide only dichotomous prognoses without specifying the expected level of recovery (Schorr et al., 2016). In contrast to amplitude and variance metrics, the potential diagnostic and prognostic value of spectral EEG connectivity metrics during task-free measurements have yet to be explored.

Several findings suggest that spectral EEG characteristics may be indicative of the level of consciousness (LoC) in patients with DOC. Compared to fully conscious control participants, patients with DOC consistently show a reduction in the amplitude of oscillations in the  $\alpha$  and  $\beta$  bands, and often show a concurrent increase in  $\theta$  and  $\delta$  amplitude (Chennu et al., 2014; Lechinger et al., 2013; Lehembre et al., 2012; Varotto et al., 2014). Furthermore, during auditory processing, entropy metrics of cortical information exchange vary monotonically across LoC (King et al., 2013; Sitt et al., 2014). These and other (Giacino et al., 2014; Laureys et al., 2000; Schiff et al., 2007) findings have been proposed to reflect discontinuities in the thalamo-cortico-thalamic circuit that disrupt large-scale functional interactions, and thereby enable local cortical properties to shape the spectral dynamics (Giacino et al., 2014; Schiff, 2010; Schiff et al., 2014). However, it is unclear to what extent such accounts capture longitudinal spectral changes across patients' recovery, because comparisons between LoC have almost exclusively been conducted using cross-sectional (between-group) designs.

Here, we report a longitudinal study in which we acquired a total of 74 task-free EEG measurements over the course of patient recovery from severe acquired brain injury. We explored the feasibility of diagnosis and prognosis of DOC within individual patients based on the amplitude and connectivity of neural oscillations, using state-of-the-art analysis methods. We found that nonlinear frequency band-specific changes in these metrics occur over the course of patients' recovery, and that these changes align well with the metrics' frequency band-specific diagnostic value. Strikingly, we found that connectivity during a single task-free EEG measurement predicted the level of patient recovery approximately 3 months later with a high level of accuracy. These results identify task-free EEG amplitude and connectivity as reliable diagnostic and prognostic markers of DOC, which can be inexpensively acquired at bedside and are completely independent of the patients' neurocognitive abilities. Furthermore, our results tentatively suggest that the preservation of reverberant thalamo-cortical interactions predicts later reemergence of consciousness, and thus may yield new insights into the neural mechanisms underlying recovery following brain injury.

## 2. Materials and methods

### 2.1. Participants

Sixteen patients (12 male) with severe brain injury, who participated in an ‘Early Intensive Neurorehabilitation Programme’ (Eilander et al., 2007; Eilander et al., 2005; Eilander et al., 2016) between November 2002 and January 2004, were included in the study. Age at the time of injury ranged from 5.5 to 25.2 years (Median = 17.6 years; SD = 4.8). Time since injury at admission ranged from 44 to 136 days (Median = 66.5 days; SD = 22.6). All but six patients suffered from traumatic brain injury caused by traffic accidents. Patients participated in the programme for 45 to 197 days (Median = 102 days; SD = 37.6). See Table 1 for a detailed description of the patients’ characteristics.

A healthy control group consisted of 16 individuals (8 male), aged from 5.8 to 25.2 years (Median = 18.33; SD = 5.8). Patients and controls did not differ in age ( $t(15) = 0.71$ ,  $p = 0.5$ ). All patients and the healthy control group participated in this study following informed consent given by one of the parents, a legal representative or partner (patients and controls younger than 16 years), or by themselves (controls of 16 years or older). The study was approved by a medical ethics committee (METTOP).

### 2.2. Observation scale

We categorized the patients’ LoC based on the definitions described by ‘the International Working Party on the Management of the Vegetative State’ (Andrews, 1996), and the Aspen Neurobehavioural Conference (Giacino, 1997; Giacino et al., 2002). The categorization describes a comatose state, three vegetative sub-states, three non-vegetative sub-states, and a conscious state (see Supplementary Table 1 for a detailed classification scheme). This classification scale, now named the Post-Acute Level of Consciousness scale (PALOC-s), has a high reliability and validity (Eilander et al., 2009). Supplementary Fig. 1 shows PALOC-s scores per measurement. Linear mixed model analysis (McLean et al., 1991) (see below) showed that PALOC-s score increased significantly ( $F(1,16) = 16.40$ ,  $p = 0.001$ ) across measurements, indicating that the patients improved over time. In a second step the PALOC-s classification was reduced to three levels: levels 1, 2, and 3 were defined as UWS, levels 4, 5, and 6 as MCS, levels 7 and 8 as exit from MCS (eMCS) or conscious state.

### 2.3. Procedure

Nine days after a patient was admitted to the treatment programme the first measurements took place. Patients were examined while they were lying in a bed in a quiet room with a constant temperature ( $23 \pm 1^\circ\text{C}$ ). Every two weeks the (eyes open) EEG measurement of 3 min took place at the same time of the day (between 10:30 a.m. and 11:30 a.m.).

Every two weeks the rehabilitation physician determined the LoC based on the categories described in Supplementary Table 1. These assessments were performed until the patient was discharged from the programme. The programme was completed when 1) a patient qualified for regular rehabilitation because of recovery of consciousness and cognitive abilities, or 2) a patient did not show any recovery for a period of at least six weeks. These different recovery courses led to a variation in time span of the patients’ participation in the study and in the number of measurements.

### 2.4. EEG collection and preprocessing

Brain activity was recorded using actively shielded pin-electrodes, by means of the ActiveTwo System (BioSemi, The Netherlands) at a sampling rate of 2 kHz. The electrodes were placed by using a head cap and electrode gel (Parker Signa) according to the 10/20 system, at F3,

Fz, F4, C3, Cz, C4, Pz, and Oz. Horizontal EOG was recorded from two electrodes placed at the outer canthi of both eyes. Vertical EOG was recorded from electrodes above and below the two eyes.

We used functions from the EEGLAB toolbox (Delorme and Makeig, 2004) and custom MATLAB code to preprocess the EEG data. First, EEG data were down-sampled the data to 1 kHz to speed up computation and rereferenced off-line to the average of the mastoid electrodes. Next, we removed line noise by applying a notch filter (50 Hz), and removed any additional high-frequency noise (e.g., harmonics of line noise) by applying a low-pass filter at 100 Hz. Additionally, we removed slow drifts related to changes in galvanic skin properties using a high-pass filter with a 0.5-Hz cut-off. All filters were two-way, least-squares, finite impulse response filters, and designed using the ‘fir1’ function in MATLAB 2012a. This type of filter does not introduce spurious phase consistency of oscillatory activity (Cohen, 2014; van den Brink et al., 2014), which can sometimes occur with infinite impulse response filters, and so will not bias connectivity estimates. After filtering, we rereferenced the pairs of vertical and horizontal EOG channels to each other, rereferenced all scalp electrodes to the common average, and segmented the data into non-overlapping epochs of 2 s duration.

Next, data segments containing artifacts were automatically detected using three criteria: the joint probability (3.5 SD cut-off), electrode kurtosis (3.5 SD cut-off), and a voltage threshold ( $\pm 100 \mu\text{V}$ ). In addition, data segments containing transient muscular activity or eye-movement-related artifacts were manually selected. On average, 14% (SD 11) of the data of the patient group and 10% (SD 2) of the data of the control group was marked as artefactual. After the rejection of artefactual segments, on average 170 s (SD 30) of clean data remained for the patient group, and 163 s (SD 8) for the control group. The amount of clean data did not differ between the patients and controls ( $t(90) = 0.99$ ,  $p = 0.33$ ), or between the different levels of consciousness within the patient group (all  $p$  values  $> 0.17$ ). A flowchart of the preprocessing steps is shown in Fig. 1.

### 2.5. Frequency band-specific amplitude

For all segments of clean EEG data we computed the fast Fourier transform (FFT). To enable the comparison of values across participants, we expressed the amplitude at each frequency as a percentage of the total spectrum (the summed activity across all frequencies), separately per electrode. We produced a metric of global frequency band-specific power by averaging FFT amplitude across electrodes and across frequencies within 4 canonical frequency bands:  $\delta$  (1–3 Hz);  $\theta$  (4–7 Hz);  $\alpha$  (8–15 Hz);  $\beta$  (16–31 Hz). In addition, we computed the ratio in amplitude between the  $\alpha$  and  $\delta$  bands, as used in earlier studies (Cheadle et al., 2014; Fellinger et al., 2011). We did not include the  $\gamma$  band because of controversy over the ability of surface EEG to reliably detect it (Yuval-Greenberg et al., 2008).

### 2.6. EEG connectivity

We used correlation of orthogonalized amplitude envelopes as our measure of EEG connectivity (Hipp et al., 2012; Siems et al., 2016). The continuous (unsegmented) data of each recording of each participant were passed through a series of band-pass filters to isolate activity within the 4 canonical frequency bands ( $\delta$ ,  $\theta$ ,  $\alpha$ , and  $\beta$ , see above). We filtered the continuous data rather than segmented data to prevent the introduction of edge artifacts that would otherwise occur around the segments’ outer bounds. We again used two-way, least-squares, finite impulse response filters to ensure that no phase shifts would occur. For each EEG electrode and frequency band ( $f$ ), excluding the segments that were previously identified as containing artifacts, we computed the complex analytic signal ( $X$ ) over time ( $t$ ) via the Hilbert transform (using the ‘hilbert’ function in MATLAB 2012a).

Given their heterogeneity in aetiology, the patients most likely differed from each other as well as from the control group in terms of

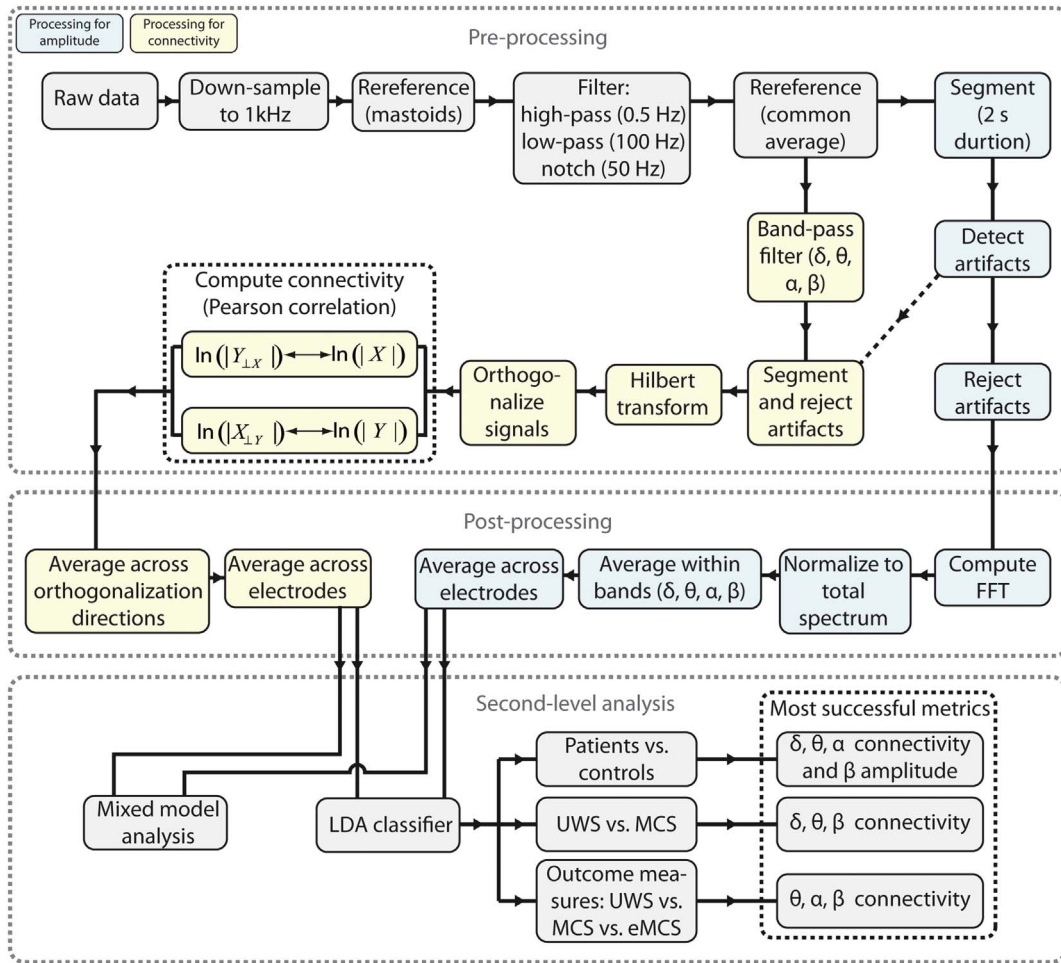


Fig. 1. Flowchart depicting all analysis steps.

volume conduction. That is, the patients' cerebral architecture is compromised, and in a way that varies across patients. Thus, the point spread of brain activity across the scalp most likely varies across patients as well. To accurately estimate connectivity across scalp electrodes, we therefore needed to account for the influence of volume conduction and differences between groups / patients therein. To do so, we adopted a previously established procedure (Hipp et al., 2012). Specifically, we orthogonalized the complex analytic signal of each electrode to that of each other electrode (Hipp et al., 2012) using the following equation:

$$Y_{\perp X}(t, f) = \text{imag} \left( Y(t, f) \frac{X(t, f)^*}{|X(t, f)|} \right),$$

where  $X, Y \in S$  and  $S$  denotes the set of analytic signals of all electrodes, and  $*$  denotes the complex conjugate.  $Y_{\perp X}(t, f)$  represents the signal  $Y$  orthogonalized to signal  $X$ , at time point  $t$  and frequency band  $f$ . For each frequency band and electrode pair we then computed the Pearson correlation coefficient between  $\ln(|Y_{\perp X}|)$  and  $\ln(|X|)$ . This can be interpreted as computing the correlation between the log-transformed orthogonalized amplitude envelopes, or in other words, the extent to which activity within canonical frequency bands co-fluctuated across brain regions. We performed the orthogonalization and correlation in both directions, from signal  $X$  to  $Y$  and from signal  $Y$  to  $X$ , yielding two correlation coefficients per electrode pair. These correlation coefficients were subsequently averaged. In all cases where correlation coefficients were averaged, we applied Fisher's r-to-z transform prior to averaging, and subsequently applied the z-to-r transform.

For each participant, this procedure resulted in a frequency band ( $\delta$ ,

$\theta$ ,  $\alpha$ ,  $\beta$ ) by electrode (F3, Fz, F4, C3, Cz, C4, Pz, Oz) by electrode (F3, Fz, F4, C3, Cz, C4, Pz, Oz) (size: 4 by 8 by 8) matrix of correlation coefficients that indicated the strength of connectivity between pairs of electrodes, corrected for the effect of volume conduction. Next, we computed a frequency band-specific metric of global brain connectivity by averaging across the lower triangular part of the connectivity matrices (excluding the diagonal). This indicated, for each frequency band, the average connectivity across all unique electrode pairs. We focus on global connectivity for three reasons. First, the number of statistical tests is greatly reduced by collapsing across electrode pairs, which alleviates the need for a stringent correction for multiple comparisons. Second, as noted above, there was substantial heterogeneity across patients in aetiology. By considering only global dynamics, our results are less likely to be dominated by idiosyncratically located focal disturbances in brain processing. Instead, the metric putatively reflects (pathological) connectivity that is shared by the entire cortex and thus captures processes that are pervasive in nature. Third, such shared cortical dynamics arguably reflect processes that have more profound consequences for patient recovery than localized effects (Schiff et al., 2014). All  $t$ -tests that involved connectivity were performed on Fisher's r-to-z transformed correlation coefficients.

To confirm that the orthogonalization procedure effectively reduced spurious correlations in the amplitude envelope across EEG electrodes, we compared the orthogonalized amplitude envelope correlation with the amplitude envelope correlation that was computed on non-orthogonalized signals, separately for each group and each frequency band, using paired sample  $t$ -tests. In other words, we computed the connectivity metrics on the data to which all preprocessing steps were



applied, except for the orthogonalization procedure. If signal orthogonalization effectively reduced spurious correlations, then the connectivity metrics that were computed using orthogonalized signals should be lower compared to connectivity metrics that were computed using non-orthogonalized signals. As expected, for both patients and control participants, the orthogonalization reduced the strength of connectivity significantly for all frequency bands (all  $p$ 's < 0.0001). Thus, the orthogonalization was effective in reducing spurious correlations.

## 2.7. Linear discriminant analysis

We used linear discriminant analysis (LDA) to explore whether frequency band-specific EEG amplitude and connectivity can be used to reliably dissociate patients with DOC from healthy control participants and from each other. That is, LDA was used to establish to what extent amplitude and connectivity metrics contain diagnostic information, at the individual patient level. In addition, we used receiver operated characteristic (ROC) analysis to examine to what extent the amplitude and connectivity of individual frequency bands contributed to the classifier. Second, we explored whether EEG amplitude and connectivity during the first measurement upon admission to the study also contain prognostic information by using LDA to predict each patient's chances of recovery.

We implemented the LDA with a naïve Bayes classifier, using the 'classify' function in MATLAB 2012a. The classifier fitted a multivariate normal density to each group with diagonal covariance matrix estimates ('diaglinear' selected as 'type'), and then used likelihood ratios to assign observations to groups. 'Groups' here refers to either patient/control, patient groups (UWS/MCS), or outcome measures (UWS/MCS/eMCS). 'Observations' refer to the features that the classifier relied on: FFT amplitude, connectivity, or a combination of both. For each classification, unless mentioned otherwise, we report the combination of features that presented the highest degree of classification accuracy, quantified as the percentage of participants that were correctly assigned to their respective group by the classifier. In all cases, classification was performed using a leave-one-out procedure. Specifically, we first trained the classifier on the whole group of participants minus one, and we then used this trained classifier to predict to which group the left-out participant belonged. We did this for each participant separately so that eventually we obtained a prediction for each participant based on the rest of the participants.

The statistical significance of classification accuracy was assessed using non-parametric permutation testing. For 10,000 iterations we shuffled the assignment of observations to groups, and repeated the leave-one-out procedure. In cases where we tested multiple combinations of features, we computed all possible combinations of features (15 possible combinations when using only amplitude or only connectivity

features, and 255 possible combinations when using both amplitude and connectivity features) in each iteration of the permutation test. This resulted in an aggregate distribution of 'accuracies' under the null hypothesis, corrected for the selection of a subset of features from the total possible feature set. We then calculated a  $p$  value (corrected for multiple comparisons across features) for the observed classification accuracy as the proportion of (aggregated) null accuracies that were more extreme than the true accuracy. Similarly, we tested the significance of the ROC analyses by comparing the area under the ROC curves to null distributions generated with permutation testing.

## 2.8. Longitudinal analyses

We used linear mixed models (McLean et al., 1991) with maximum likelihood estimation to assess changes in spectral amplitude and connectivity over the course of patient recovery. In other words, we used linear mixed models to examine within-participant changes in amplitude and connectivity across patient recovery, and assessed the statistical significance of these changes at the group-level. Mixed models are ideally suited for repeated-measures designs with a varying number of samples per participant. We tested linear, exponential, and quadratic models with random slopes and intercepts across the 3 LoCs (UWS, MCS, and eMCS), with both the participants and LoC as random factors, and amplitude/connectivity as dependent variables. In each instance of the statistical test, we selected the covariance model that minimized the Akaike information criterion (Akaike, 1974) and Bayesian information criterion (Schwarz, 1978), and therefore provided the best fit. All mixed-model analyses were conducted using SPSS Statistics 23.

## 3. Results

### 3.1. Global and broad-band EEG activity distinguishes patients with DOC from controls, and from each other

We collected a total of 74 task-free EEG measurements at bedside from 16 patients diagnosed with DOC, using the Post-Acute Level of Consciousness scale (PALOC-s) (Eilander et al., 2009), and an additional 16 measurements from healthy age- and education-matched control participants. Table 1 summarizes the demographics of the patient population and the number of measurements per patient. Our first objective was to characterize group-level differences in spectral activity between patients and controls. To do so, we compared global spectral amplitude and connectivity during each patient's first measurement after entering the study to healthy controls, using independent-sample  $t$ -tests. Compared to healthy control participants, the patients showed an increased amplitude of oscillations in the  $\delta$  and  $\theta$  bands, but reduced amplitude in the  $\alpha$  and  $\beta$  bands (Fig. 2A;  $\delta$ :  $t(30) = 2.83$ ,  $p = 0.004$ ;  $\theta$ :  $t(30) = 2.20$ ,  $p = 0.018$ ;  $\alpha$ :  $t(30) = -3.17$ ,  $p = 0.002$ ;  $\beta$ :  $t(30)$

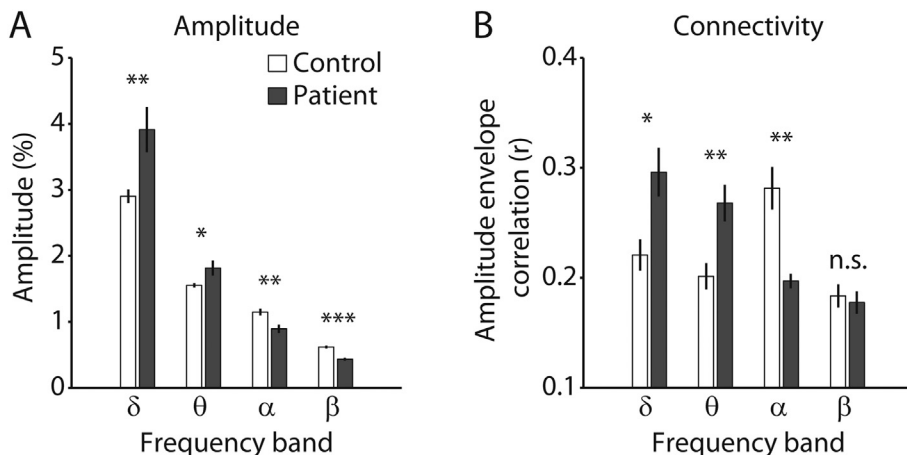


Fig. 2. Global spectral amplitude and connectivity. A) Amplitude per frequency band for each group. B) Connectivity per frequency band for each group. Error bars denote the SEM. \* $p < 0.05$ ; \*\* $p < 0.01$ ; \*\*\* $p < 0.001$ ; n.s. nonsignificant.

$= -6.14, p < 0.001$ ). The group-collapsed full amplitude spectrum is shown in Supplementary Fig. 2. Supplementary Fig. 3 shows midline spectra for each measurement of each patient, and includes the LoC per measurement. Similar to increased low-frequency amplitude, the patients showed hypersynchronous activity in the  $\delta$  and  $\theta$  bands, and hyposynchronous activity in the  $\alpha$  band (Fig. 2B;  $\delta$ :  $t(15) = 2.51, p = 0.02$ ;  $\theta$ :  $t(15) = 2.95, p = 0.01$ ;  $\alpha$ :  $t(15) = -3.94, p = 0.001$ ;  $\beta$ :  $t(15) = -0.38, p = 0.71$ ). Thus, compared to controls, the patients showed pronounced differences in both amplitude and connectivity that spanned a wide spectral range. Such global spectral disturbances in patients with DOC are consistent with earlier reports (Chennu et al., 2014; Lechinger et al., 2013; Lehenbre et al., 2012; Varotto et al., 2014), and are indicative of widespread pathophysiological cortical activity.

Our next objective was to determine to what extent spectral amplitude and connectivity (Fig. 1) can aid the diagnosis of DOC at the level of individual patients. To do this, we used a naïve Bayes classifier. The classifier relied on frequency band-specific amplitude, connectivity, or a combination thereof, to predict the group of each individual (patient or control). The statistical significance of classifier accuracy was assessed with permutation testing. When using amplitude in all frequency bands to distinguish the patients from participants in the control group, the classifier performed with an accuracy of 81% (26 out of 32 individuals assigned to the correct group,  $p < 0.001$ ). Second, classification based on connectivity in the  $\delta, \theta$ , and  $\alpha$  bands was also highly accurate (88%, 28 out of 32 participants correctly assigned,  $p < 0.0001$ ). When the classifier relied on connectivity in the  $\delta, \theta$ , and  $\alpha$  bands, and was additionally informed by amplitude in the  $\beta$  band, accuracy was highest (94%, 30 out of 32 participants correctly assigned,  $p < 0.0001$ ). Fig. 3A shows the confusion matrix for classification based on both amplitude and connectivity features. These results indicate that both spectral amplitude and connectivity can readily be used as metrics to distinguish patients from controls, but the combination of the two types of metrics yields additional information that cannot be inferred from either type of metric in isolation. ROC analysis indicated that the amplitude of all individual frequency bands contributed to the classifier, with the  $\beta$  band showing the highest accuracy (Fig. 3B, top row). Moreover, connectivity in all but the  $\beta$  band contributed to the classifier (Fig. 3B, bottom row).

A useful clinical diagnostic tool for the diagnosis of DOC does not

only distinguish patients from controls, but also provides a reliable indication of the type of DOC within individual patients. Thus, we next set out to investigate to what extent a classifier could distinguish patients that were diagnosed with UWS from those that showed minimal signs of consciousness (MCS). These two types of DOC are most difficult to dissociate based on EEG metrics alone (Schurger et al., 2015), so classification of these two types of DOC provides a good benchmark to test the diagnostic value of amplitude and connectivity. Moreover, the longitudinal study design enabled us to sample an adequate number of measurements at these two LoC from within the patient group to be used for classification.

A classifier that relied on connectivity in the  $\delta, \theta$ , and  $\alpha$  bands and amplitude in the  $\beta$  band, identical to the features used above, showed modest but above-chance-level performance in distinguishing the two groups (75% accurate,  $p = 0.018$ ). However, accuracy improved when the classifier only used connectivity in the  $\delta, \theta$  and  $\beta$  bands as features (85% accurate,  $p = 0.001$ , Fig. 4A). Thus, connectivity alone was most informative when distinguishing UWS patients from those patients that displayed minimal signs of consciousness. In agreement with this notion, ROC analysis showed that only connectivity in the  $\delta, \theta$  and  $\beta$  bands contributed to the classifier (Fig. 4B). Control analyses ruled out patient age as a confound, and explored the contribution of individual EEG electrodes to the overall pattern of results (see Supplementary Results). As noted above, for distinguishing patients from fully conscious control participants, the combination of amplitude and connectivity proved to be most informative. Together, these findings raise the hypothesis that changes in amplitude occur when patients transitioned from unconsciousness to consciousness, but changes in connectivity occur at the transition from UWS to MCS. To address this hypothesis, in the next section we explore longitudinal changes in oscillatory amplitude and connectivity metrics across the patients' course of recovery.

### 3.2. Frequency band-specific amplitude and connectivity track longitudinal changes in patients' level of consciousness

Having established that spectral amplitude and connectivity can be used as reliable markers for the diagnosis of DOC, we next set out to investigate whether spectral amplitude and connectivity track the LoC over the course of patients' recovery. In the following set of analyses, we used linear mixed models to test if the individual metrics changed

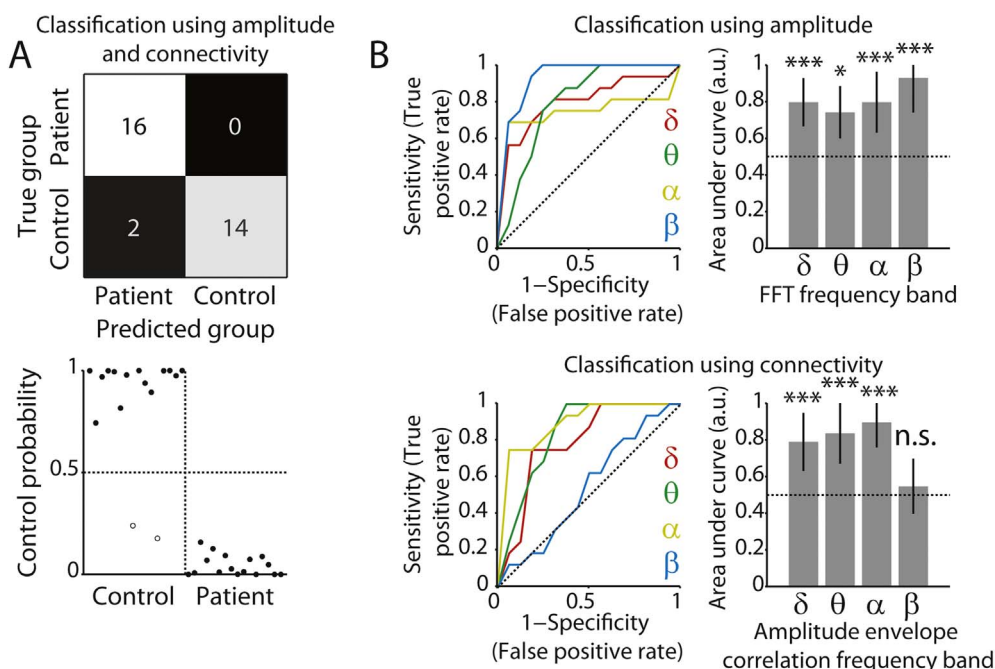


**Fig. 3.** Classification of patients and controls. A) Top row, confusion matrix for classification distinguishing patients from controls, based on both amplitude ( $\beta$  band) and connectivity ( $\delta, \theta, \alpha$  bands). Colors indicate the relative number of cases in each cell. Bottom row, associated classifier weights. Filled and open dots show correctly and incorrectly classified individuals, respectively. B) ROC curves and corresponding areas under the curve, indicating the extent to which each frequency band contributed to the classifier. Top row, for spectral amplitude. Bottom row, for amplitude envelope correlations. The area under the curve can be interpreted as the accuracy with which the individual participant/patient's group can be predicted based on the metric in that frequency band. The horizontal dotted line indicates chance performance. Error bars denote the 95% confidence interval of the permuted null distribution. \* $p < 0.05$ ; \*\*\* $p < 0.001$ ; n.s. non-significant.

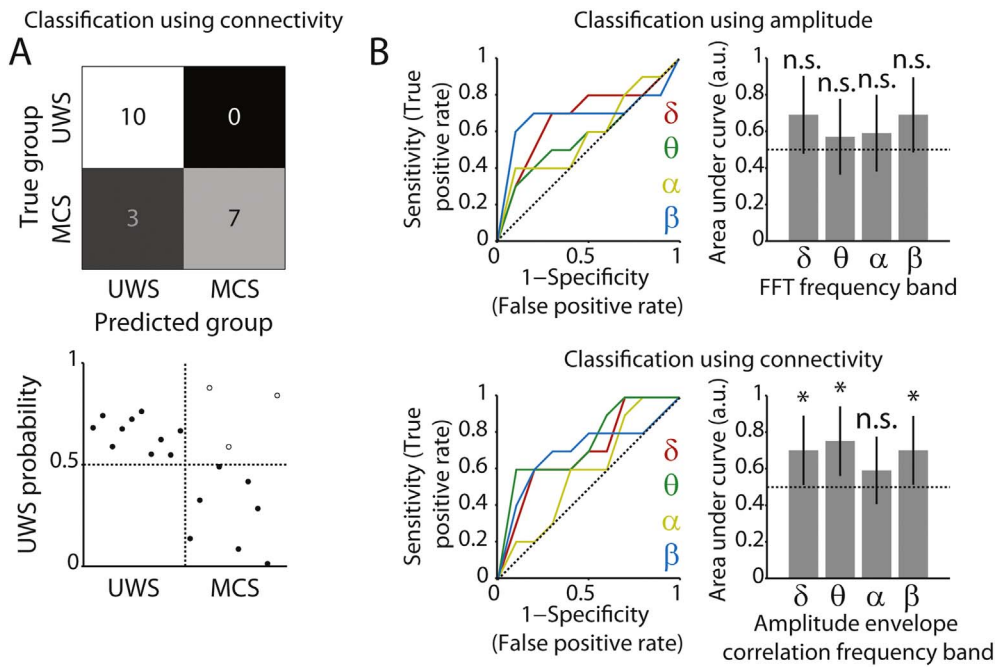


**Fig. 4.** Classification between patient groups. A) Top row, confusion matrix for classification distinguishing UWS from MCS patients, based on connectivity ( $\delta$ ,  $\theta$ ,  $\beta$  bands). Colors indicate the relative number of cases in each cell. Bottom row, associated classifier weights. Filled and open dots show correctly and incorrectly classified patients, respectively. B) ROC curves and corresponding areas under the curve, indicating the extent to which each frequency band contributed to the classifier. Top row, for spectral amplitude. Bottom row, for amplitude envelope correlations. The area under the curve can be interpreted as the accuracy with which the individual participant/patient's group can be predicted based on the metric in that frequency band. The horizontal dotted line indicates chance performance. Error bars denote the 95% confidence interval of the permuted null distribution. \* $p < 0.05$ ; \*\*\* $p < 0.001$ ; n.s. non-significant.

across the LoC. We explored linear, exponential, and quadratic changes in all frequency bands. Furthermore, we examined changes in the ratio between  $\alpha$  and  $\delta$  amplitude, as used in prior research (Cheadle et al., 2014; Fellinger et al., 2011). The amplitude and connectivity of all frequency bands for each LoC are shown in Supplementary Fig. 4 and Supplementary Fig. 5.

The ratio between  $\alpha$  and  $\delta$  amplitude increased significantly across LoC ( $F(2,23) = 4.63$ ,  $p = 0.021$ ). As shown in Fig. 5A, however, the data suggested that this increase was not linear over time, but instead was relatively stable for lower LoC and then exponentially increased, resulting in an overshoot compared to the control group. Consistent with this notion, including an exponential predictor in the model resulted in a significant exponential effect of LoC on  $\alpha/\delta$  amplitude ratio ( $F(1,32) = 6.31$ ,  $p = 0.017$ ), and rendered the linear effect non-significant ( $F(1,40) = 3.40$ ,  $p = 0.073$ ). Thus, the change in the  $\alpha/\delta$  amplitude ratio across LoC was best captured by an exponential increase instead of by a linear increase. Similarly,  $\beta$  amplitude increased linearly with LoC ( $F(2,21) = 3.75$ ,  $p = 0.040$ ), but an exponential model best explained the change across LoC ( $F(1,14) = 11.42$ ,  $p = 0.005$ ; Fig. 5B). As opposed to a progressive increase across LoC, connectivity in the  $\theta$  band showed a quadratic relationship with LoC ( $F(1,45) = 9.05$ ,  $p = 0.024$ ). Fig. 5C shows that  $\theta$  connectivity was low for UWS scores, increased for MCS scores, and recovered to normative levels for eMCS scores. No single patient was responsible for the group-

level pattern of results, as excluding each individual patient did not change the main findings. In the following, we explore whether amplitude and connectivity also provide prognostic information.

### 3.3. Brain-wide connectivity predicts patient recovery

Thus far we have shown that global amplitude and connectivity can be used as markers for the diagnosis of DOC. Furthermore, frequency band-specific changes in these metrics occur across the course of patient recovery. We next asked if amplitude and connectivity can also be used as reliable prognostic markers. That is, can amplitude and connectivity during a single task-free EEG measurement, conducted upon the patients' admission to the study, be used to predict the patients' level of recovery? To do this, we used a classifier to predict each patient's outcome diagnosis at the point of discharge from the rehabilitation center. The outcome diagnosis was either UWS, MCS, or eMCS, and thus chance-level classification accuracy was 33%.

When amplitude was used as features, the  $\alpha$  band alone yielded the highest classification accuracy (62% accurate,  $p = 0.014$ ). In line with the observations made above, amplitude dissociated relatively well between MCS and eMCS, but performed poorly at dissociating the lower LoC outcome measures (Fig. 6A). However, connectivity in the  $\theta$ ,  $\alpha$  and  $\beta$  bands proved to be more reliable features, resulting in an accuracy of 75% ( $p < 0.001$ , Fig. 6B). Connectivity in isolation also out-performed

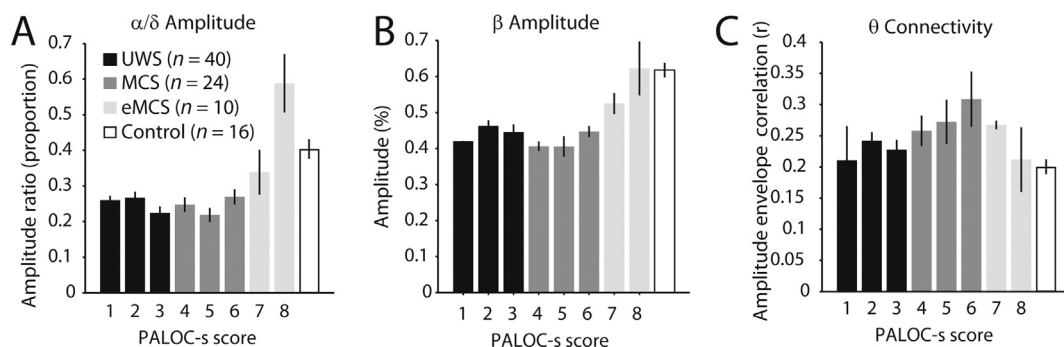


**Fig. 5.** Longitudinal changes in EEG metrics. A) The ratio between  $\alpha$  and  $\theta$  amplitude increases with level of consciousness, and shows an overshoot for the patients with higher levels of consciousness. The number of measurements per level of consciousness is indicated by  $n$ . B)  $\beta$  amplitude increases with level of consciousness. C)  $\theta$  connectivity shows an inverted-U relationship with level of consciousness. Controls are shown for visual comparison. Error bars denote the SEM. PALOC-s: Post-Acute Level of Consciousness scale.

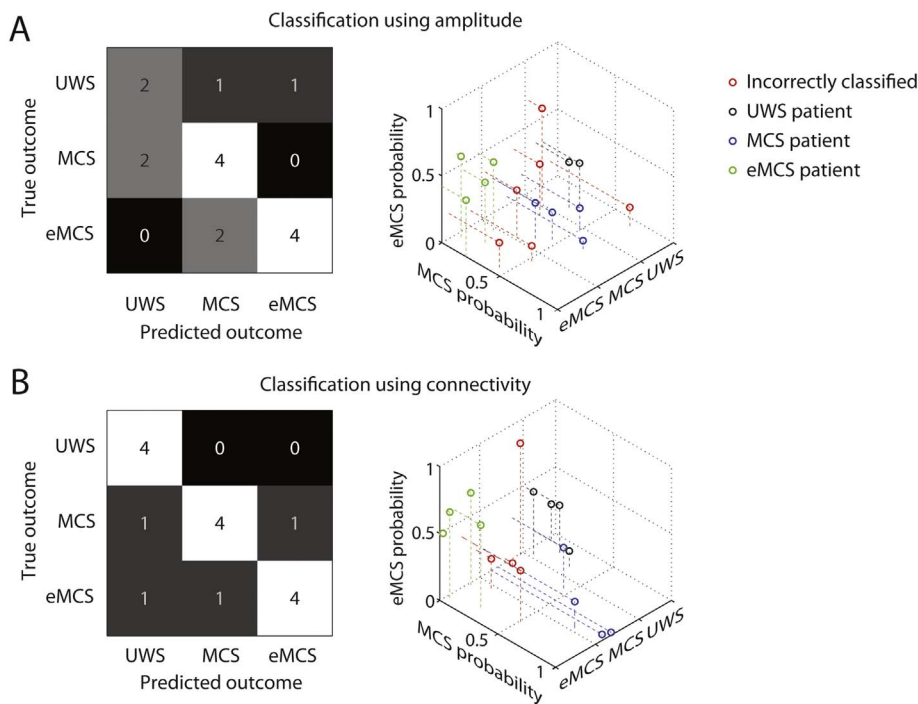


**Fig. 6.** Classification of outcome measures. A) Confusion matrix for classification using  $\alpha$  amplitude (left), and associated classifier weights (right). B) Confusion matrix for classification using  $\theta$ ,  $\alpha$  and  $\beta$  connectivity (left), and associated classifier weights (right). Shades of grey and numbers in the confusion matrices indicate the relative number of cases in each cell.

a classifier that relied on both amplitude and connectivity (69% accuracy,  $p = 0.003$ ). Thus, based on connectivity during a single task-free EEG measurement, conducted upon the patients' admission to the study, it was possible to make a prognosis for patient recovery  $\sim 3$  months later with 75% accuracy. The possibility that variation across patients in LoC at the time of measurement was driving the classifier cannot account for our findings, because LoC during the first measurement and outcome score were not significantly correlated ( $r = 0.33$ ,  $p = 0.21$ ). Additional control analyses ruled out patient age as a confound (see Supplementary Results). These results identify EEG connectivity as a reliable marker of recovery from DOC. As we discuss below, these results also tentatively point to neural mechanisms that may underlie recovery from DOC.

#### 4. Discussion

In the present study, we examined if and how task-free spectral EEG amplitude and connectivity metrics change over the course of patient recovery, following severe brain injury. Moreover, we examined if these metrics can be used to predict the current (diagnosis) and future (prognosis) LoC of individual patients. Our first key finding is that amplitude and connectivity can reliably be used as diagnostic markers of DOC (Figs. 3 and 4). Dissociating patients from healthy control participants worked best when relying on  $\delta$ ,  $\theta$ , and  $\alpha$  band connectivity, and amplitude in the  $\beta$  band. Dissociating UWS from MCS patients was most successful based on  $\delta$ ,  $\theta$  and  $\beta$  band connectivity. Our second key finding is that task-free spectral amplitude and connectivity do not vary monotonically across LoC, but instead show nonlinear dynamics (Fig. 5). Specifically, we found that amplitude in the  $\beta$  band, and  $\alpha/\delta$  amplitude ratio, increased exponentially across LoC, while  $\theta$  band connectivity showed an inverted-U relationship with LoC. Finally, our findings show that connectivity metrics ( $\theta$ ,  $\alpha$  and  $\beta$  bands) are highly robust markers of patient prognosis (Fig. 6B).

The exponential increase in amplitude (ratio) across LoC is broadly consistent with an account that posits that consciousness recovers only after neural function crosses a critical threshold level (Bagnato et al., 2013). Moreover, the inverted-U shaped relationship between LoC and  $\theta$  connectivity may explain why amplitude and connectivity provide complementary diagnostic information when dissociating patients from

controls, whereas connectivity alone is most informative when dissociating UWS from MCS patients. Whereas amplitude (ratio) is stable for UWS/MCS and then increases,  $\theta$  connectivity deviates most strongly in MCS, but appears normative for UWS and eMCS. Accordingly, the three LoC are each marked by a unique spectral fingerprint (Siegel et al., 2012) that is apparent only when both amplitude and connectivity are considered. This suggests that a successful distinction between the three LoC requires multivariate classification, as we have used here.

A recent account has highlighted the central role of the thalamus in the regulation of arousal through its excitatory connections to the cortex and striatum (Schiff, 2010; Schiff et al., 2014). According to this account, pathologically elevated slow-wave amplitude indicates damage in the thalamo-cortico-thalamic loop. Such damage in the thalamo-cortical system causes a loss of excitatory drive to the cortex and consequently results in a general 'slowing down' of cortical rhythms (Giacino et al., 2014; Schiff et al., 2014), consistent with our findings (Fig. 2a) and animal models of cortical deafferentation (Lemieux et al., 2014; Timofeev et al., 2000). Importantly, combined with the finding of absent pathologically increased connectivity in UWS (Fig. 5C), the pattern of results speculatively suggests a lack of central thalamic coordination of oscillatory activity across the cortex in UWS, potentially due to the loss of excitatory drive from the thalamus to the cortex, or vice versa. Relatedly, the inverted-U shaped pattern of  $\theta$  connectivity across LoC may explain why connectivity metrics in particular were most informative about later patient recovery. Elevated  $\theta$  connectivity in UWS patients might be indicative of the relative sparing of projections within the thalamo-cortico-thalamic circuit, and hence the potential for recovery of reverberant excitatory drive and associated high-frequency activity (Laureys et al., 2000; Rosanova et al., 2012; Schiff et al., 2007). However, future research is needed to probe the relationship between the here observed spectral disturbances and thalamo-cortical interactions, as we did not examine such a relationship directly. Nevertheless, the notion that the preservation of thalamo-cortico-thalamic interactions may underlie the recovery of awareness is consistent with findings that the recovery of consciousness is paralleled by a restoration in thalamo-cortical interactions (Laureys et al., 2000), the spread of cortical activity following transcranial magnetic stimulation dissociates UWS from MCS patients (Casali et al., 2013; Rosanova



et al., 2012), and thalamic stimulation can facilitate behavioral responsiveness (Schiff et al., 2007).

Notwithstanding the potential diagnostic and prognostic utility of amplitude and connectivity metrics, some limitations of the present study should be acknowledged. First, the classifier's false negative rate for the purpose of diagnosis as well as for prognosis was higher than the false positive rate (Fig. 3, Fig. 4, Fig. 6), indicating that the classifier was somewhat pessimistic. Ideally, the false positive and false negative rates would be balanced. False negatives in diagnosis based on behavioral criteria have been attributed in part to temporal fluctuations in the patient's arousal state (Piarulli et al., 2016). This may also be the case for the neural markers employed here. This potential problem could be resolved by close monitoring of ultradian fluctuations in the patients' arousal state (Piarulli et al., 2016). Additionally, in the current study we relied on behavioral scores to assess the diagnostic and prognostic utility of EEG markers, but diagnosis using behavioral criteria may be suboptimal (Giacino et al., 2014). Future studies may further validate the here employed EEG markers by for example using a range of diagnostic criteria. Second, the nonlinear variations in amplitude and connectivity observed here (Fig. 5) appear to be at odds with earlier reports of monotonic changes across LoC in entropy metrics of cortical interactions (King et al., 2013; Sitt et al., 2014). This discrepancy may be explained by the fact that in these studies patients were presented with auditory stimuli, which could evoke synchronous cortical states. Alternatively, the here employed measure of connectivity (orthogonalized amplitude envelope correlations) may reflect qualitatively different network interactions than the metrics used in previous studies. Third, it should be noted that our findings may not generalize to DOC with different aetiology (e.g., due to neurodegenerative disease). Finally, due to the exploratory nature of the current study, our findings strongly call for independent replication, preferably with a larger sample size, to determine the specific combination of features that yields the most accurate diagnosis and prognosis.

In conclusion, diagnosis and prognosis based on amplitude and connectivity from task-free EEG measurements is feasible. These measures can be acquired inexpensively, with low electrode density, at bedside, and are fully independent of the patients' neurocognitive abilities. Our longitudinal findings in the amplitude domain are consistent with an existing account that proposes that neural function crosses a threshold level prior to the reemergence of consciousness following DOC (Bagnato et al., 2013). Furthermore, our findings in the connectivity domain lend support to a recent account that posits that dysfunction in the thalamo-cortical system underlies DOC (Schiff, 2010; Schiff et al., 2014), and further suggest that neural signatures of thalamo-cortical interactions are predictive of patient recovery. A rigorous assessment of the pathophysiological mechanisms underlying DOC may open the door to diagnostic taxonomies that are independent of behavioral criteria, and facilitate early targeted interventions that are tailored to the individual patient's needs.

## Conflict of interests

The authors declare no competing financial interests.

## Acknowledgements

This work was funded by a Consolidator Grant of the European Research Council (grant number GA 283314-NOREPI); Stichting Centraal Fonds RVVZ, Zeist; Hersenstichting Nederland, Den Haag; Johanna KinderFonds, Arnhem; CZ Groep Zorgverzekeringen Fonds vrijwillige verzekeringen, Sittard; Zorgverzekeraar VGZ Fonds vrijwillige verzekeringen, Tilburg; Zorg en Zekerheid, Leiden; and Stichting Bio-Kinderrevalidatie, Arnhem. The funding agencies had no role in study design; in the collection, analysis and interpretation of data; in the writing of the report; and in the decision to submit the article for publication.

## Appendix A. Supplementary data

Supplementary data to this article can be found online at <https://doi.org/10.1016/j.nicl.2017.10.003>.

## References

- Akaike, H., 1974. New look at statistical-model identification. *IEEE Trans. Autom. Control* 19, 716–723.
- Andrews, K., 1996. International working party on the management of the vegetative state: summary report. *Brain Inj.* 10, 797–806.
- Bagnato, S., Boccagni, C., Sant'angelo, A., Fingelkurts, A.A., Galardi, G., 2013. Emerging from an unresponsive wakefulness syndrome: brain plasticity has to cross a threshold level. *Neurosci. Biobehav. Rev.* 37, 2721–2736.
- Boly, M., Garrido, M.I., Gosseries, O., Bruno, M.A., Boveroux, P., Schnakers, C., Massimini, M., Litvak, V., Laureys, S., Friston, K., 2011. Preserved feedforward but impaired top-down processes in the vegetative state. *Science* 332, 858–862.
- van den Brink, R.L., Wynn, S.C., Nieuwenhuis, S., 2014. Post-error slowing as a consequence of disturbed low-frequency oscillatory phase entrainment. *J. Neurosci.* 34, 11096–11105.
- Casali, A.G., Gosseries, O., Rosanova, M., Boly, M., Sarasso, Simone, Casali, K.R., Casarotto, S., Bruno, M.-A., Laureys, S., Tononi, G., Massimini, M., 2013. A theoretically based index of consciousness independent of sensory processing and behavior. *Sci. Transl. Med.* 5, 198ra105.
- Cheadle, S., Wyart, V., Tsetsos, K., Myers, N., de Gardelle, V., Herce Castanon, S., Summerfield, C., 2014. Adaptive gain control during human perceptual choice. *Neuron* 81, 1429–1441.
- Chennu, S., Fioino, P., Kamau, E., Allanson, J., Williams, G.B., Monti, M.M., Noreika, V., Arnatkeviciute, A., Canales-Johnson, A., Olivares, F., Cabezas-Soto, D., Menon, D.K., Pickard, J.D., Owen, A.M., Bekinschtein, T.A., 2014. Spectral signatures of re-organised brain networks in disorders of consciousness. *PLoS Comput. Biol.* 10, e1003887.
- Cohen, M., 2014. *Analyzing Neural Time Series Data: Theory and Practice*. MIT, Cambridge, MA.
- Delorme, A., Makeig, S., 2004. EEGLAB: an open source toolbox for analysis of single-trial EEG dynamics including independent component analysis. *J. Neurosci. Methods* 134, 9–21.
- Demertzi, A., Antonopoulos, G., Heine, L., Voss, H.U., Crone, J.S., de Los Angeles, C., Bahri, M.A., Di Perri, C., Vanhaudenhuyse, A., Charland-Verville, V., Kronbichler, M., Trinka, E., Phillips, C., Gomez, F., Tshibanda, L., Soddu, A., Schiff, N.D., Whitfield-Gabrieli, S., Laureys, S., 2015. Intrinsic functional connectivity differentiates minimally conscious from unresponsive patients. *Brain* 138, 2619–2631.
- Eilander, H.J., Wijnen, V.J., Scheirs, J.G., de Kort, P.L., Prevo, A.J., 2005. Children and young adults in a prolonged unconscious state due to severe brain injury: outcome after an early intensive neurorehabilitation programme. *Brain Inj.* 19, 425–436.
- Eilander, H.J., Timmerman, R.B., Scheirs, J.G., Van Heugten, C.M., De Kort, P.L., Prevo, A.J., 2007. Children and young adults in a prolonged unconscious state after severe brain injury: long-term functional outcome as measured by the DRS and the GOSE after early intensive neurorehabilitation. *Brain Inj.* 21, 53–61.
- Eilander, H.J., van de Wiel, M., Wijers, M., van Heugten, C.M., Buljevac, D., Lavrijsen, J.C., Hoenderdaal, P.L., de Letter-van, der, Heide, L., Wijnen, V.J., Scheirs, J.G., de Kort, P.L., Prevo, A.J., 2009. The reliability and validity of the PALOC-s: a post-acute level of consciousness scale for assessment of young patients with prolonged disturbed consciousness after brain injury. *Neuropsychol. Rehabil.* 19, 1–27.
- Eilander, H.J., Wijnen, V.J., Schouten, E.J., Lavrijsen, J.C., 2016. Ten-to-twelve years after specialized neurorehabilitation of young patients with severe disorders of consciousness: a follow-up study. *Brain Inj.* 30, 1302–1310.
- Estraneo, A., Loreto, V., Guarino, I., Boemia, V., Paone, G., Moretta, P., Trojano, L., 2016. Standard EEG in diagnostic process of prolonged disorders of consciousness. *Clin. Neurophysiol.* 127, 2379–2385.
- Fellinger, R., Klimesch, W., Schnakers, C., Perrin, F., Freunberger, R., Gruber, W., Laureys, S., Schabus, M., 2011. Cognitive processes in disorders of consciousness as revealed by EEG time-frequency analyses. *Clin. Neurophysiol.* 122, 2177–2184.
- Fischer, C., Luaute, J., Morlet, D., 2010. Event-related potentials (MMN and novelty P3) in permanent vegetative or minimally conscious states. *Clin. Neurophysiol.* 121, 1032–1042.
- Giacino, J.T., 1997. Disorders of consciousness: differential diagnosis and neuropathologic features. *Semin. Neurol.* 17, 105–111.
- Giacino, J.T., Ashwal, S., Childs, N., Cranford, R., Jennett, B., Katz, D.I., Kelly, J.P., Rosenberg, J.H., Whyte, J., Zafonte, R.D., Zasler, N.D., 2002. The minimally conscious state: definition and diagnostic criteria. *Neurology* 58, 349–353.
- Giacino, J.T., Fins, J.J., Laureys, S., Schiff, N.D., 2014. Disorders of consciousness after acquired brain injury: the state of the science. *Nat. Rev. Neurol.* 10, 99–114.
- Hipp, J.F., Hawellek, D.J., Corbetta, M., Siegel, M., Engel, A.K., 2012. Large-scale cortical correlation structure of spontaneous oscillatory activity. *Nat. Neurosci.* 15, 884–890.
- Höller, Y., Bergmann, J., Kronbichler, M., Crone, J.S., Schmid, E.V., Golaszewski, S., Ladurner, G., 2011. Preserved oscillatory response but lack of mismatch negativity in patients with disorders of consciousness. *Clin. Neurophysiol.* 122, 1744–1754.
- Jennett, B., Plum, F., 1972. Persistent vegetative state after brain damage: a syndrome in search of name. *Lancet* 1, 734–737.
- King, J.R., Sitt, J.D., Faugeras, F., Rohaut, B., El Karoui, I., Cohen, L., Naccache, L., Dehaene, S., 2013. Information sharing in the brain indexes consciousness in non-communicative patients. *Curr. Biol.* 23, 1914–1919.
- Kotchoubey, B., Lang, S., Mezger, G., Schmalohr, D., Schneek, M., Semmler, A., Bostanov,

- V., Birbaumer, N., 2005. Information processing in severe disorders of consciousness: vegetative state and minimally conscious state. *Clin. Neurophysiol.* 116, 2441–2453.
- Laureys, S., Faymonville, M.E., Luxen, A., Lamy, M., Franck, G., Maquet, P., 2000. Restoration of thalamocortical connectivity after recovery from persistent vegetative state. *Lancet* 355, 1790–1791.
- Laureys, S., Owen, A.M., Schiff, N.D., 2004. Brain function in coma, vegetative state, and related disorders. *Lancet Neurol.* 3, 537–546.
- Lechinger, J., Bothe, K., Pichler, G., Michitsch, G., Donis, J., Klimesch, W., Schabus, M., 2013. CRS-R score in disorders of consciousness is strongly related to spectral EEG at rest. *J. Neurol.* 260, 2348–2356.
- Lehembre, R., Bruno, M.-A., Vanhaudenhuyse, A., Chatelle, C., Cologan, V., Leclercq, Y., Soddu, A., Marcq, B., Laureys, S., Noirhomme, Q., 2012. Resting-state EEG study of comatose patients: a connectivity and frequency analysis to find differences between vegetative and minimally conscious states. *Funct. Neurol.* 27, 41–47.
- Lemieux, M., Chen, J.Y., Lonjers, P., Bazhenov, M., Timofeev, I., 2014. The impact of cortical deafferentation on the neocortical slow oscillation. *J. Neurosci.* 34, 5689–5703.
- McLean, R.A., Sanders, W.L., Stroup, W.W., 1991. A unified approach to mixed linear models. *Am. Stat.* 45, 54–64.
- Monti, M.M., Vanhaudenhuyse, A., Coleman, M.R., Boly, M., Pickard, J.D., Tshibanda, L., Owen, A.M., Laureys, S., 2010. Willful modulation of brain activity in disorders of consciousness. *N. Engl. J. Med.* 362, 579–589.
- Owen, A.M., Coleman, M.R., Boly, M., Davis, M.H., Laureys, S., Pickard, J.D., 2006. Detecting awareness in the vegetative state. *Science* 313, 1402.
- Piarulli, A., Bergamasco, M., Thibaut, A., Cologan, V., Gosseries, O., Laureys, S., 2016. EEG ultradian rhythmicity differences in disorders of consciousness during wakefulness. *J. Neurol.* 263, 1746–1760.
- Rosanova, M., Gosseries, O., Casarotto, S., Boly, M., Casali, A.G., Bruno, M.A., Mariotti, M., Boveroux, P., Tononi, G., Laureys, S., Massimini, M., 2012. Recovery of cortical effective connectivity and recovery of consciousness in vegetative patients. *Brain* 135, 1308–1320.
- Schiff, N.D., 2010. Recovery of consciousness after brain injury: a mesocircuit hypothesis. *Trends Neurosci.* 33, 1–9.
- Schiff, N.D., Giacino, J.T., Kalmar, K., Victor, J.D., Baker, K., Gerber, M., Fritz, B., Eisenberg, B., Biondi, T., O'Connor, J., Kobylarz, E.J., Farris, S., Machado, A., McCagg, C., Plum, F., Fins, J.J., Rezaei, A.R., 2007. Behavioural improvements with thalamic stimulation after severe traumatic brain injury. *Nature* 448, 600–603.
- Schiff, N.D., Nauvel, T., Victor, J.D., 2014. Large-scale brain dynamics in disorders of consciousness. *Curr. Opin. Neurobiol.* 25, 7–14.
- Schorr, B., Schlee, W., Arndt, M., Bender, A., 2016. Coherence in resting-state EEG as a predictor for the recovery from unresponsive wakefulness syndrome. *J. Neurol.* 263, 937–953.
- Schurger, A., Sarigiannidis, I., Naccache, L., Sitt, J.D., Dehaene, S., 2015. Cortical activity is more stable when sensory stimuli are consciously perceived. *Proc. Natl. Acad. Sci. U. S. A.* 112, E2083–2092.
- Schwarz, G., 1978. Estimating dimension of a model. *Ann. Stat.* 6, 461–464.
- Siegel, M., Donner, T.H., Engel, A.K., 2012. Spectral fingerprints of large-scale neuronal interactions. *Nat. Rev. Neurosci.* 13, 121–134.
- Siems, M., Pape, A.A., Hipp, J.F., Siegel, M., 2016. Measuring the cortical correlation structure of spontaneous oscillatory activity with EEG and MEG. *NeuroImage* 129, 345–355.
- Sitt, J.D., King, J.R., El Karoui, I., Rohaut, B., Faugeras, F., Gramfort, A., Cohen, L., Sigman, M., Dehaene, S., Naccache, L., 2014. Large scale screening of neural signatures of consciousness in patients in a vegetative or minimally conscious state. *Brain* 137, 2258–2270.
- Stender, J., Mortensen, K.N., Thibaut, A., Darkner, S., Laureys, S., Gjedde, A., Kupers, R., 2016. The minimal energetic requirement of sustained awareness after brain injury. *Curr. Biol.* 26, 1494–1499.
- Timofeev, I., Grenier, F., Bazhenov, M., Sejnowski, T.J., Steriade, M., 2000. Origin of slow cortical oscillations in deafferented cortical slabs. *Cereb. Cortex* 10, 1185–1199.
- Varotto, G., Fazio, P., Rossi Sebastiano, D., Duran, D., D'Incerti, L., Parati, E., Sattin, D., Leonardi, M., Franceschetti, S., Panzica, F., 2014. Altered resting state effective connectivity in long-standing vegetative state patients: an EEG study. *Clin. Neurophysiol.* 125, 63–68.
- Wijnen, V.J., van Boxtel, G.J., Eilander, H.J., de Gelder, B., 2007. Mismatch negativity predicts recovery from the vegetative state. *Clin. Neurophysiol.* 118, 597–605.
- Yuval-Greenberg, S., Tomer, O., Keren, A.S., Nelken, I., Deouell, L.Y., 2008. Transient induced gamma-band response in EEG as a manifestation of miniature saccades. *Neuron* 58, 429–441.